

ARTICLE



Hypoxic exosomal HIF-1 α -stabilizing circZNF91 promotes chemoresistance of normoxic pancreatic cancer cells via enhancing glycolysis

Zhu Zeng^{1,4}, Yong Zhao^{1,4}, QingYong Chen^{1,4}, Shuai Zhu^{1,4}, Yi Niu², Zeng Ye¹, Ping Hu¹, Ding Chen¹, Peng Xu¹, Jinghuang Chen¹, Chaojie Hu¹, Yuhang Hu¹, Fengyu Xu¹, Jiang Tang¹, Fan Wang¹, Shengbo Han¹, Mengqi Huang¹, Chunyou Wang³ and Gang Zhao¹✉

© The Author(s), under exclusive licence to Springer Nature Limited 2021

Research has indicated that hypoxia profoundly contributes to chemoresistance of pancreatic cancer (PC), while the precise mechanism has not been fully elucidated. In this study, we report a hypoxic exosomal circular RNA (circRNA)-mediated mechanism of conferred chemoresistance in PC cells. Gemcitabine (GEM) resistance was enhanced in normoxic PC cells incubated with exosomes derived from hypoxic PC cells. CircRNA microarray displayed that circZNF91 was remarkably increased in hypoxic exosomes of PC cells compared with normoxic exosomes. Overexpression of circZNF91 obviously stimulated chemoresistance in PC cells, while knockdown of circZNF91 retarded the hypoxic exosome-transmitted chemoresistance. Mechanistically, the hypoxic-induced exosomal circZNF91 transmitted into normoxic PC cells could competitively bind to miR-23b-3p, which deprives the inhibition of miR-23b-3p on expression of deacetylase Sirtuin1 (SIRT1). Consequently, the upregulated SIRT1 enhanced deacetylation-dependent stability of HIF-1 α protein, leading to glycolysis and GEM chemoresistance of recipient PC cells. In addition, we revealed that the increased circZNF91 in hypoxic exosome was attributed to the transcriptional regulation by HIF-1 α . Coincidentally, transmission of hypoxic exosomes into subcutaneous xenografts in nude mice obviously facilitated the chemoresistance of transplanted PC tumor, which could be reversed by depletion of circZNF91 or upregulation of miR-23b-3p. Furthermore, clinical data showed that circZNF91 was significantly upregulated in PC tissues and correlated with overexpression of glycolytic enzymes and short overall survival time. Collectively, exosomal circZNF91 can function as a cargo mediating the signal transmission between hypoxic and normoxic tumor cells to promote GEM chemoresistance of PC and may potentially serve as a therapeutic target.

Oncogene (2021) 40:5505–5517; <https://doi.org/10.1038/s41388-021-01960-w>

INTRODUCTION

Pancreatic cancer (PC) is a devastating malignant disease with a 5-year survival rate of less than 8% due to the early symptom concealment, delayed diagnosis, and insensitivity to chemoradiotherapy [1, 2]. Only 10~15% of the total number of patients can be surgically treated [3–5]. Efforts to improve the survival, especially those with advanced PC, mainly focus on adjuvant chemotherapy [6, 7]. At present, the chemotherapy regimen for PC is mainly Gemcitabine (GEM) or a combination regimen based on GEM. However, PC had obvious innate and acquired resistance to GEM with clinical application, which significantly reduced its efficacy [8, 9]. Exploration of chemoresistance mechanism of PC cells is conducive to discovery more efficient drug formulations and schemes, improving overall survival rate of patients.

Drug resistance is tightly associated with hypoxia [10]. Overexpression of HIF-1 α in human solid tumors is closely related to radiotherapy and chemotherapy resistance [11, 12]. Studies have

shown that on the one hand, HIF-1 α may increase the ability of PC cells to transport chemotherapy drugs by inducing expression of drug-resistant proteins; On the other hand, HIF-1 α may inhibit apoptosis induced by chemotherapy drugs by upregulating Bcl-2 and downregulating Bax [13, 14]. In addition, research showed that MUC1-mediated HIF-1 α stabilization facilitates GEM resistance via metabolic reprogramming in PC, and targeting HIF-1 α could reverse the resistance [15]. Hence, it is of profound significance to elucidate the mechanism by which HIF-1 α functions in resistance of PC cells to GEM for improving drug resistance.

Exosomes, as the current hotspot of oncology research, participate in occurrence and development of PC, and induce the formation of immune tolerance and chemotherapy resistance [16]. Increasing evidence has indicated that exosomal circRNAs dysregulation is correlated with chemoresistance. Studies clarified that exosomes, secreted by temozolomide resistant cells, contributed to temozolomide resistance of sensitive cancer cells by

¹Department of Emergency Surgery, Union Hospital, Tongji Medical College, Huazhong University of Science and Technology, Wuhan, China. ²Department of Gastrointestinal Surgery, Union Hospital, Tongji Medical College, Huazhong University of Science and Technology, Wuhan, China. ³Department of Pancreatic Surgery, Union Hospital, Tongji Medical College, Huazhong University of Science and Technology, Wuhan, China. ⁴These authors contributed equally: Zhu Zeng, Yong Zhao, QingYong Chen, Shuai Zhu ✉email: gangzhao@hust.edu.cn

transferring CircNFI [17]. In addition, oxaliplatin-resistant cell-derived exosomes delivered circular RNA to sensitive cells to promote glycolysis and drug resistance of colorectal cancer cells [18]. The study of exosomes in chemotherapy resistance of PC is of great value in treatment and prognosis of PC, while there are few studies on exosomes and chemotherapy resistance of PC.

Here, we found that both CM and exosomes from hypoxic PC cells significantly enhanced GEM resistance of normoxic PC cells. Subsequently, results from circRNA microarray demonstrated that circZNF91 was obviously accumulated in hypoxic exosomes. Meanwhile, both in vitro and in vivo experiments validated exosomal circZNF91 as a key modulator in regulating GEM resistance of normoxic PC cells. The following experiments revealed that circZNF91 was transcriptionally upregulated by HIF-1 α , while such increased exosomal circZNF91 could be delivered into recipient normoxic cells and stabilize HIF-1 α protein, thereby enhancing glycolysis and drug resistance of PC cells.

RESULTS

CircZNF91 is critical for the hypoxic exosome-promoted GEM resistance in normoxic cancer cells

Hypoxia has been confirmed to contribute to chemoresistance [19, 20]. Our results validated that cells cultured under hypoxia displayed a remarkably increased IC50 when treated with GEM compared with cells cultured under normoxia (Supplementary Fig. S1a). Meanwhile, cells co-cultured with hypoxic PC cells exhibited poorer response to GEM than those co-cultured with normoxic cells (Supplementary Fig. S1b), indicating that hypoxic PC cells promoted resistance of normoxic PC cells. Then we cultured PC cells under normoxia or hypoxia for 48 h, and collected the medium as normoxic CM/hypoxic CM. The results showed that cells cultured under hypoxic CM had an increased IC50 upon GEM (Supplementary Fig. S1c), suggesting that hypoxic CM might contain promoting factor conferring chemoresistance to normoxic PC cells.

Considering the vital roles of exosomes in the interaction between cancer cells, we hypothesized that exosomes were involved in the chemoresistance transmission. Electron microscopy revealed that hypoxic cancer cells secreted more exosomes than normoxic cancer cells (Fig. 1a). Moreover, exosome marker CD63 and the absence of Golgi compartment-specific marker GM130 confirmed the identity of exosomes (Fig. 1b). Using fluorescent dye PKH26 to label exosomes, we verified that hypoxic exosomes could be fused to recipient normoxic cells (Fig. 1c and Supplementary Fig. S1d). Moreover, cells fed with hypoxic exosomes displayed a significantly increased IC50 and enhanced anchorage-independent growth with GEM treatment (Supplementary Fig. S1e, f). These results indicated that hypoxic PC cell-derived exosomes could enhance GEM resistance of normoxic PC cells.

To clarify whether circRNA could exert considerable influence on recipient cells, we applied microarray assay to analyze differentiated circRNAs between normoxic exosomes and hypoxic exosomes (Fig. 1d). Compared to normoxic exosomes, 470 annotated circRNAs (log2 fold change >2) were upregulated and 448 annotated circRNAs (log2 fold change <-2) were downregulated in hypoxic exosomes. Among these upregulated circRNAs in hypoxic exosomes, we focused on circZNF91 for further research (Fig. 1e). In order to certify circZNF91 was a circRNA, we designed two sets of primers in RT-qPCR: divergent primers, amplifying circular form, and convergent primers, amplifying linear form. The results showed that circZNF91 was detected by divergent primers in cDNA but not in genomic DNA (gDNA) of PANC-1, BxPC-3, and SW1990 cells (Supplementary Fig. S2a). In addition, circRNA did not contain poly (A) tail, circZNF91 could not be detected in cDNA of oligo-dT primers. Consistently,

circZNF91 was obviously detected in cDNA of random primers (Supplementary Fig. S2b). The results validated that circZNF91 was elevated in PANC-1, BxPC-3, and SW1990 cells compared to human pancreatic duct epithelial cells (Supplementary Fig. S2c). In addition, circZNF91 was localized mainly in cytoplasm (Supplementary Fig. S2d, e). Then we compared exosomal RNA with total RNA isolated from CM, there was little difference in content, but RNA in CM with exosomes dislodged was hard to detect (Supplementary Fig. S2f). Further exploration indicated that circZNF91 expression in PC cell-divided exosomes did not change in response to exonuclease ribonuclease R (RNase R) treatment with or without Triton X-100 (Supplementary Fig. S2g). More importantly, circZNF91 was more resistant to RNase R digestion than ZNF91 and GAPDH mRNA (Supplementary Fig. S2h). In addition, the result displayed that circZNF91 was more stable than linear ZNF91 in BxPC-3 cells (Supplementary Fig. S2i). Consistent with the result of microarray, circZNF91 was upregulated in hypoxic exosomes of PC cells (Fig. 1f). Therefore, these results suggested that hypoxic PC cells might confer circZNF91 to normoxic cells via exosomes loading.

Next, three short interfering RNAs were designed to explore the functional role of circZNF91 (Supplementary Fig. S3a). The results showed that knockdown circZNF91 inhibited GEM resistance in PC cells, but did not affect mRNA expression of ZNF91 (Supplementary Fig. S3b, c). To further validate circZNF91 function, we established a vector-based system to overexpress circZNF91. CircZNF91 overexpression significantly increased the production of circZNF91 in PC cells without any changes in ZNF91 mRNA expression, but promoted GEM resistance remarkably. Moreover, ZNF91 overexpression did not affect circZNF91 expression nor the GEM resistance (Supplementary Fig. S3d–f). In addition, in vivo results showed that mice in LV-siCircZNF91 group displayed enhanced sensitivity to GEM compared to control group, which was reversed via upregulating CircZNF91 (Supplementary Fig. S3g, h). Exosomes secreted from circZNF91-overexpressed or hypoxic PC cells obviously enhanced circZNF91 expression and GEM resistance in recipient PC cells, but exosomes secreted from hypoxic PC cells did not promote the content of circZNF91 and GEM resistance in circZNF91-downregulated PC cells (Fig. 1g, h). Collectively, these results clarified a critical role of circZNF91 in regulating GEM resistance.

In order to validate the critical role of exosomes, we reduced the production of exosomes by depletion of RAB27A/B (Supplementary Fig. S4a) or inhibiting neutral sphingomyelinase-2 (NSMase) with GW4869 [21, 22]. The results indicated that there was no significant change in cell viability and intracellular circZNF91 level of PC cells after RAB27A/B downregulation or NSMase inhibition (Supplementary Fig. S4b, c). However, the number of exosomes and circZNF91 expression in CM decreased significantly (Fig. 1i and Supplementary Fig. S4d). Notably, inhibition the release of exosomes by RAB27A/B knockdown or GW4869 obviously suppressed hypoxic CM-mediated transmission of GEM resistance in PC cells, but could be rescued by exosomes derived from hypoxic and circZNF91-overexpressed PC cells (Fig. 1j, k and Supplementary Fig. S4e, f). Together, these results indicate a vital role of exosomal circZNF91 in GEM resistance transmission between hypoxic PC cells and normoxic PC cells.

Exosomal circZNF91 functions as a sponge of miR-23b-3p

Next, we sought to clarify the underlying mechanism of exosomal circZNF91 driving chemoresistance of PC cells. It has been reported that circZNF91 had a great number of Ago2 binding sites and several miRNAs target sites [23]. The binding between circZNF91 and Ago protein was validated by RNA Immunoprecipitation (RIP) assay (Fig. 2a). Among these miRNAs, miR-23b-3p has 24 target sites (Fig. 2b). Thereby, we presumed whether circZNF91 exerted its function by sponging miR-23b-3p. Our results revealed that overexpression or knockdown circZNF91

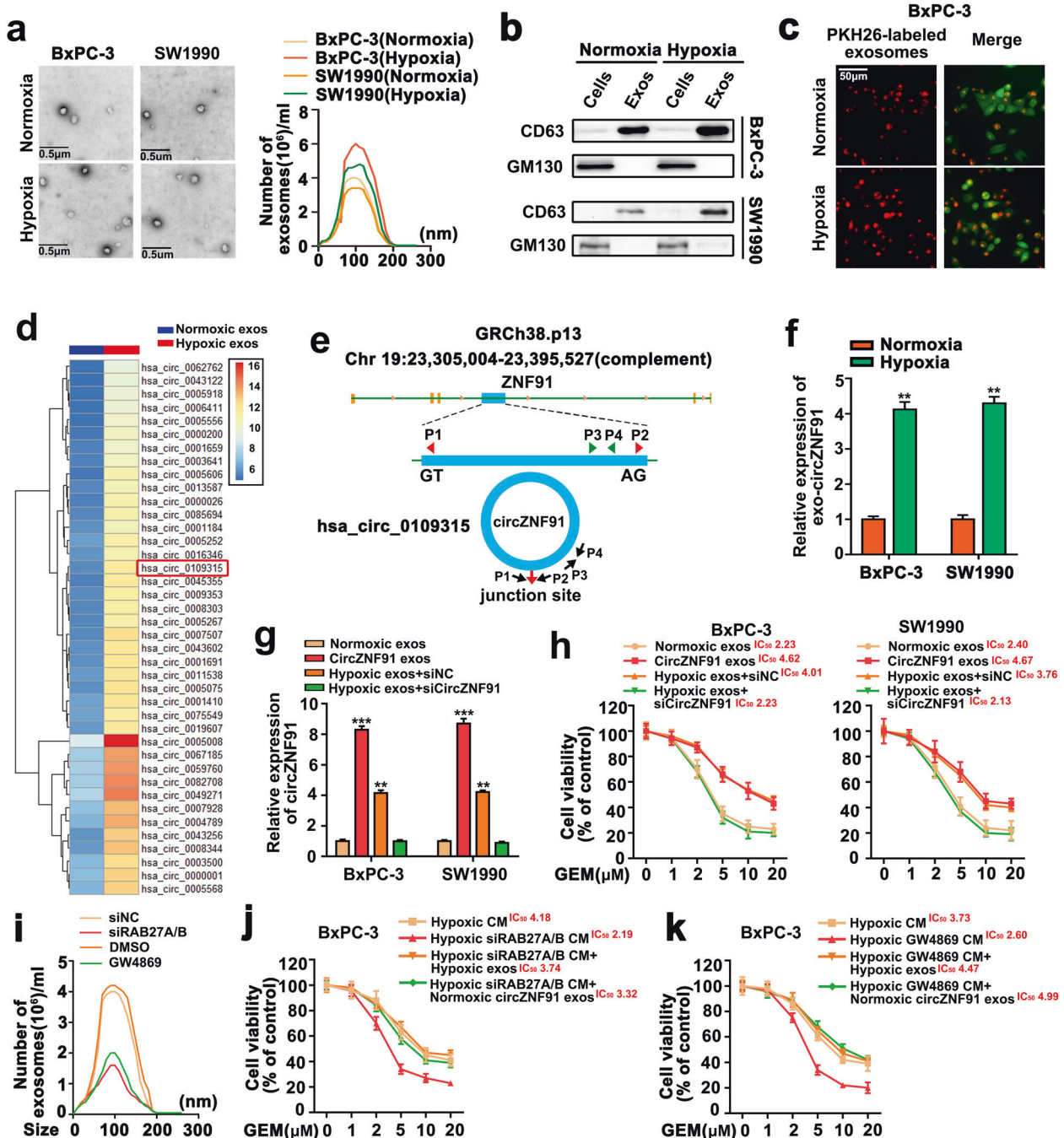


Fig. 1 CircZNF91 is critical for the hypoxic exosome-promoted GEM resistance in normoxic cancer cells. **a** (Left) Representative electron microscopy images of exosomes secreted by BxPC-3/SW1990 cells cultured under normoxia or hypoxia. (Right) NanoSight particle-tracking analysis of the size distribution and number of exosomes. **b** Western blot assay analyzed the exosome marker CD63 and GM130 in the protein extracted from cells and exosomes. **c** Exosomes were labeled with PKH26, and BxPC-3 cells were transfected lentivirus with stable expression of GFP. Incubation BxPC-3 cells with PKH26-labeled exosomes for 6 h. **d** Microarray analysis for circRNAs was conducted with exosomes derived from BxPC-3 cells cultured under normoxia or hypoxia. The heatmap displayed 40 most upregulated circRNAs. **e** Schematic illustration of circZNF91. **f** The expression of circZNF91 was detected by RT-qPCR in exosomes derived from BxPC-3 and SW1990 cells cultured under normoxia or hypoxia for 48 h. **g**, **h** BxPC-3/SW1990 cells were treated with exosomes derived from normoxic or circZNF91-overexpressed BxPC-3/SW1990 cells (circZNF91 exos); as well as exosomes derived from hypoxic BxPC-3/SW1990 cells, which were followed by transfection of siCircZNF91 (hypoxic exos + siCircZNF91) or control (hypoxic exos + siNC). The expression of circZNF91 was detected by RT-qPCR (**g**). MTT assay detected the cell viability of those pre-treated BxPC-3/SW1990 cells followed by GEM treatment at indicated concentrations for 48 h. The value of IC₅₀ was shown as indicated (**h**). **i** NanoSight particle-tracking analysis of the size distribution and number of exosomes. **j**, **k** BxPC-3 cells were pre-incubated with CM from hypoxic BxPC-3 cells, hypoxic BxPC-3 cells treated with siRAB27A/B (**j**) or GW4869 (**k**), which followed by treatment of exosomes derived from hypoxic BxPC-3 cells or circZNF91-overexpressed BxPC-3 cells. MTT assay detected the cell viability of these pre-treated BxPC-3 cells with GEM treatment at indicated concentrations for 48 h. The value of IC₅₀ was shown as indicated. Results were shown as mean ± SD of at least three independent experiments. **p < 0.01, ***p < 0.001.

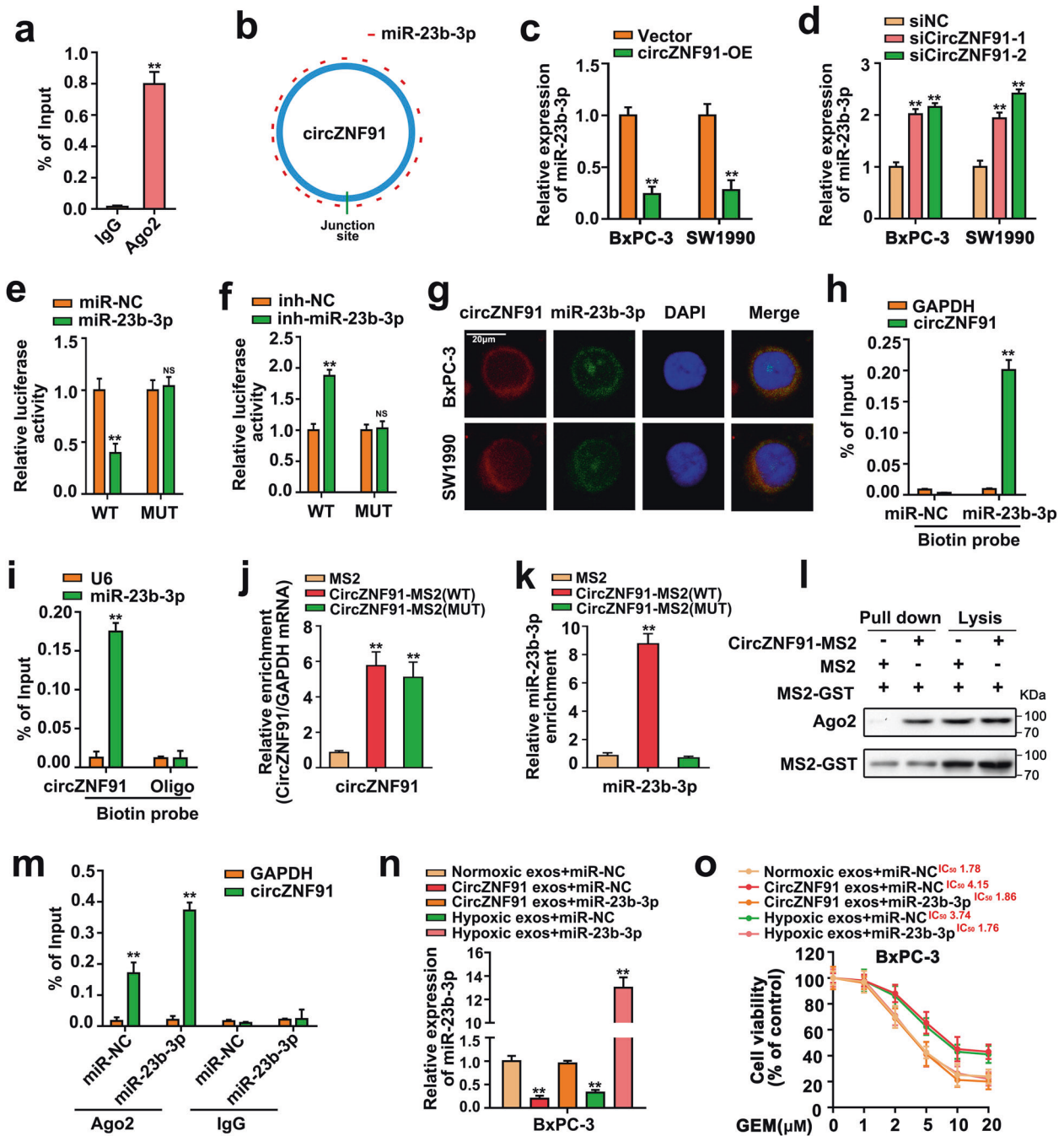


Fig. 2 Exosomal circZNF91 functions as a sponge of miR-23b-3p. **a** RIP assay of the enrichment of circZNF91 on Ago2 relative to IgG in BxPC-3 cells. **b** Schematic model presenting the potential binding sites of miR-23b-3p on circZNF91. **c, d** The expression of miR-23b-3p was detected by RT-qPCR in BxPC-3/SW1990 cells with circZNF91 overexpression (**c**) or knockdown (**d**). **e, f** BxPC-3 cells transfected with pRL-TK plasmid encoding Renilla luciferase and luciferase reporter plasmid encoding firefly luciferase and circZNF91 sequence containing wild or mutant type of miR-23b-3p binding sites followed by co-transfection of miR-NC, inh-NC, or inh-miR-23b-3p, respectively. Firefly luciferase activity was detected and normalized by Renilla luciferase activity. **g** RNA-FISH assay indicating the co-localization of circZNF91 (red) and miR-23b-3p (green) in BxPC-3/SW1990 cells. Scale bar: 20 μm. **h** Biotin-based pull-down assay detected the enrichment of circZNF91 on biotinylated miR-NC and miR-23b-3p probe. The mRNA of GAPDH served as control. **i** Biotin-based pull-down assay detected the enrichment of miR-23b-3p on biotinylated circZNF91 and Oligo probe. U6 served as control. **j, k** RT-qPCR assay analyzed circZNF91 (**j**) and miR-23b-3p (**k**) trapped by MS2. BxPC-3 cells were transfected with plasmid of MS2, circZNF91-MS2 (WT), or circZNF91-MS2 (MUT) for 48 h, then we used glutathione-SH (GSH) agarose beads to trap MS2 in cells lysate to do pull-down assay. **l** Western blot assay analyzed the expression of Ago2 in the MS2 trap assay. **m** RIP assay explored the enrichment of circZNF91 on Ago2 relative to IgG in BxPC-3 cells transfected with miR-NC or miR-23b-3p. **n, o** BxPC-3 cells were pre-treated with exosomes derived from normoxic or circZNF91-overexpressed BxPC-3 cells, as well as hypoxic exosomes that were followed by transfection of miR-23b-3p mimic or control. The expression of miR-23b-3p was detected by RT-qPCR in those pre-treated BxPC-3 cells (**n**). MTT assay detected the cell viability of those pre-treated BxPC-3 cells followed by GEM treatment at indicated concentrations for 48 h (**o**). The value of IC₅₀ was shown as indicated. Results were shown as mean ± SD of at least three independent experiments. ***p* < 0.01.

could remarkably downregulate or upregulate miR-23b-3p expression (Fig. 2c, d).

Then we sought to validate the direct interaction between circZNF91 and miR-23b-3p. The luciferase reporters carrying predicted miR-23b-3p targeting region of circZNF91 (wild type, WT) or mutated region (mutated type, MUT) were transfected into BxPC-3 cells (Supplementary Tables S1 and S2). The results showed that luciferase activity was decreased upon miR-23b-3p overexpression and increased upon miR-23b-3p inhibition in cells transfected with WT-circZNF91 plasmid (Fig. 2e, f), indicating the binding between circZNF91 and miR-23b-3p. Consistently, FISH and biotin-based pulldown assay validated the interaction between circZNF91 and miR-23b-3p (Fig. 2g–i). Since MS2-TRAP (MS2-tagged RNA affinity purification) assay was an efficient method to verify RNA-RNA interaction, we tagged wild-type and mutant-type sequence of circZNF91 with MS2 RNA hairpins as indicated method [24]. CircZNF91 was intensively trapped in cells overexpression of circZNF91-MS2 (WT or MUT), but scarcely any circZNF91 trapped in cells overexpression of MS2 only (Fig. 2j and Supplementary Fig. S5a). We also found that circZNF91-MS2 (WT) could trap miR-23b-3p in BxPC-3 cells but circZNF91-MS2 (MUT) could not (Fig. 2k). Moreover, Ago2, a core RISC (RNA-induced silencing complex) component, was detected in cells overexpression of circZNF91-MS2 (WT) (Fig. 2l). RIP assay results suggested that miR-23b-3p overexpression led to increased enrichment of circZNF91 on Ago2 (Fig. 2m), indicating that circZNF91 served as a binding platform for miR-23b-3p and Ago2.

Moreover, results demonstrated that miR-23b-3p significantly impeded GEM resistance of PC cells, and circZNF91 overexpression abrogated this effect (Supplementary Fig. S5b, c). Likewise, GEM resistance of PC cells, promoted by exosomes secreted from circZNF91-overexpressed PC cells or hypoxic PC cells, was remarkably inhibited by miR-23b-3p upregulation (Fig. 2n, o and Supplementary Fig. S5d, e). These results implied that miR-23b-3p was involved in exosomal circZNF91-transmitted chemoresistance between hypoxic PC cells and normoxic PC cells by binding to circZNF91.

CircZNF91 upregulates SIRT1 expression via competitively binding to miR-23b-3p

Using online software (PicTar, PITA, and miRanda), SIRT1 was predicted as a potential target of miR-23b-3p (Fig. 3a). Since SIRT1 was reported to be closely related to GEM resistance and tumorigenesis in PC [25, 26], and was a direct target of miR-23b-3p [27, 28], we further identified whether SIRT1 was a critical target of circZNF91/miR-23b-3p. The results showed that circZNF91 overexpression and hypoxic exosomes significantly increased the mRNA and protein level of SIRT1, which could be reversed by miR-23b-3p upregulation (Fig. 3b, c). Furthermore, a similar trend was achieved in detection of SIRT1 transcript stability after using ActD in BxPC-3 cells to block RNA synthesis (Fig. 3d, e). To further corroborate that miR-23b-3p directly bind to SIRT1 3'UTR and circZNF91 could affect the combination, luciferase reporters carrying WT or MUT versions of SIRT1 3' UTR sequences were transfected into cells along with circZNF91 overexpression plasmid/hypoxic exosomes treatment and miR-23b-3p overexpression. The results showed that circZNF91 overexpression and hypoxic exosomes markedly increased WT-3'UTR-SIRT1 but not MUT-3'UTR-SIRT1 reporter luciferase activity, while miR-23b-3p overexpression could abrogate the increase (Fig. 3f, g). Besides, MS2-TRAP assay showed that SIRT1 was intensively trapped in cells overexpression of 3'UTR-SIRT1-MS2 (WT or MUT), but scarcely any SIRT1 trapped in cells overexpression MS2 only (Fig. 3h). The result also suggested that SIRT1-MS2 (WT) could trap miR-23b-3p but SIRT1-MS2 (MUT) could not (Fig. 3i). Meanwhile, we tested Ago2 protein in MS2-trapped lysate and Ago2 was detected in SIRT1-MS2 (WT) (Fig. 3j). RIP results showed that miR-23b-3p

overexpression led to increased enrichment of Ago2 on SIRT1 transcripts (Fig. 3k). In addition, the results showed that knock-down SIRT1 could reverse the effect of circZNF91 and hypoxic exosomes on enhancing the chemoresistance of PC cells (Fig. 3l, m). Collectively, these findings suggested that circZNF91 upregulates SIRT1 expression by competitively binding to miR-23b-3p.

Exosomal circZNF91 stabilizes HIF-1 α protein by SIRT1-dependent deacetylation

Studies have shown that SIRT1 stabilizes HIF-1 α protein via deacetylation [29], we further presumed whether circZNF91/miR-23b-3p/SIRT1 pathway could regulate HIF-1 α stability. Coincidentally, our results showed that circZNF91 knockdown remarkably decreased, while circZNF91 overexpression increased HIF-1 α protein level without effects on mRNA level (Supplementary Fig. S6a, b). Meanwhile, the results showed that circZNF91 overexpression and hypoxic exosomes remarkably increased HIF-1 α protein stability in BxPC-3/SW1990 cells (Fig. 4a, b). Besides, the proteasome inhibitor, MG132, abolished the increase of HIF-1 α induced by circZNF91 overexpression or hypoxic exosomes (Fig. 4c, d). Meanwhile, the Co-immunoprecipitation (Co-IP) assay indicated that both circZNF91 overexpression and hypoxic exosomes could increase the binding between HIF-1 α and SIRT1 and decreased the acetylation of HIF-1 α , while miR-23b-3p overexpression could eliminate this effect (Fig. 4e, f). Consistently, circZNF91 overexpression and hypoxic exosomes obviously increased HIF-1 α protein level in PC cells, which was remarkably reversed by miR-23b-3p overexpression without effects on mRNA expression of HIF-1 α (Fig. 4g, h). Taken together, the results suggested that hypoxic exosomal circZNF91 enhanced GEM resistance of normoxic PC cells by promoting miR-23b-3p/SIRT1-mediated stability of HIF-1 α protein.

Hypoxic exosomal circZNF91 promotes GEM resistance of normoxic PC cells by enhancing HIF-1 α -regulated glycolysis

Studies have shown that HIF-1 α and HIF-1 α -enhanced glycolysis are related to chemoresistance [30]. Thus, we ought to know whether hypoxic exosomal HIF-1 α -stabilizing circZNF91 could increase drug resistance by increasing the glycolysis. As expected, hypoxia exosomes elevated glucose consumption, lactate production, and decreased extracellular pH value, while circZNF91 knockdown could abolish the effect (Fig. 5a–c and Supplementary Fig. S7a–c). Furthermore, the chromatin immunoprecipitation (ChIP) assay showed that the promoter of glycolytic enzymes, including GLUT1, LDHA, HK2, and PKM2, had an increased enrichment of HIF-1 α in hypoxic exosome-treated PC cells, which was reversed by circZNF91 depletion (Fig. 5d). Accordingly, both mRNA and protein levels of GLUT1, LDHA, HK2, and PKM2 were remarkably increased in hypoxic exosome-treated PC cells, which could be reversed by downregulating circZNF91 (Fig. 5e, f and Supplementary Fig. S7d, e). To further validate the role of HIF-1 α -associated glycolysis in GEM resistance transmission, we utilized Digoxin [31], YC-1 [32], or siRNA-HIF-1 α to inhibit the activity of HIF-1 α . Results showed that inhibition of HIF-1 α activity significantly prohibited the hypoxic exosome-induced glycolytic genes expression and GEM resistance in normoxic PC cells (Fig. 5g, h and Supplementary Fig. S7f, g). In addition, 2-DG, the glycolysis inhibitor, also remarkably eliminated glycolysis and GEM resistance promoted by exosomes derived from hypoxic or circZNF91-overexpressed PC cells (Fig. 5i–k and Supplementary Fig. S7h–j).

Consistently, miR-23b-3p upregulation remarkably inhibited the glucose consumption and lactate production, which was eliminated by SIRT1 overexpression (Supplementary Fig. S8a, b). More importantly, mRNA and protein levels of glycolytic enzymes and HIF-1 α protein were dramatically decreased in miR-23b-3p overexpression cells, which was restored via SIRT1 upregulation (Supplementary Fig. S8c, d). Thus, those results elucidated that

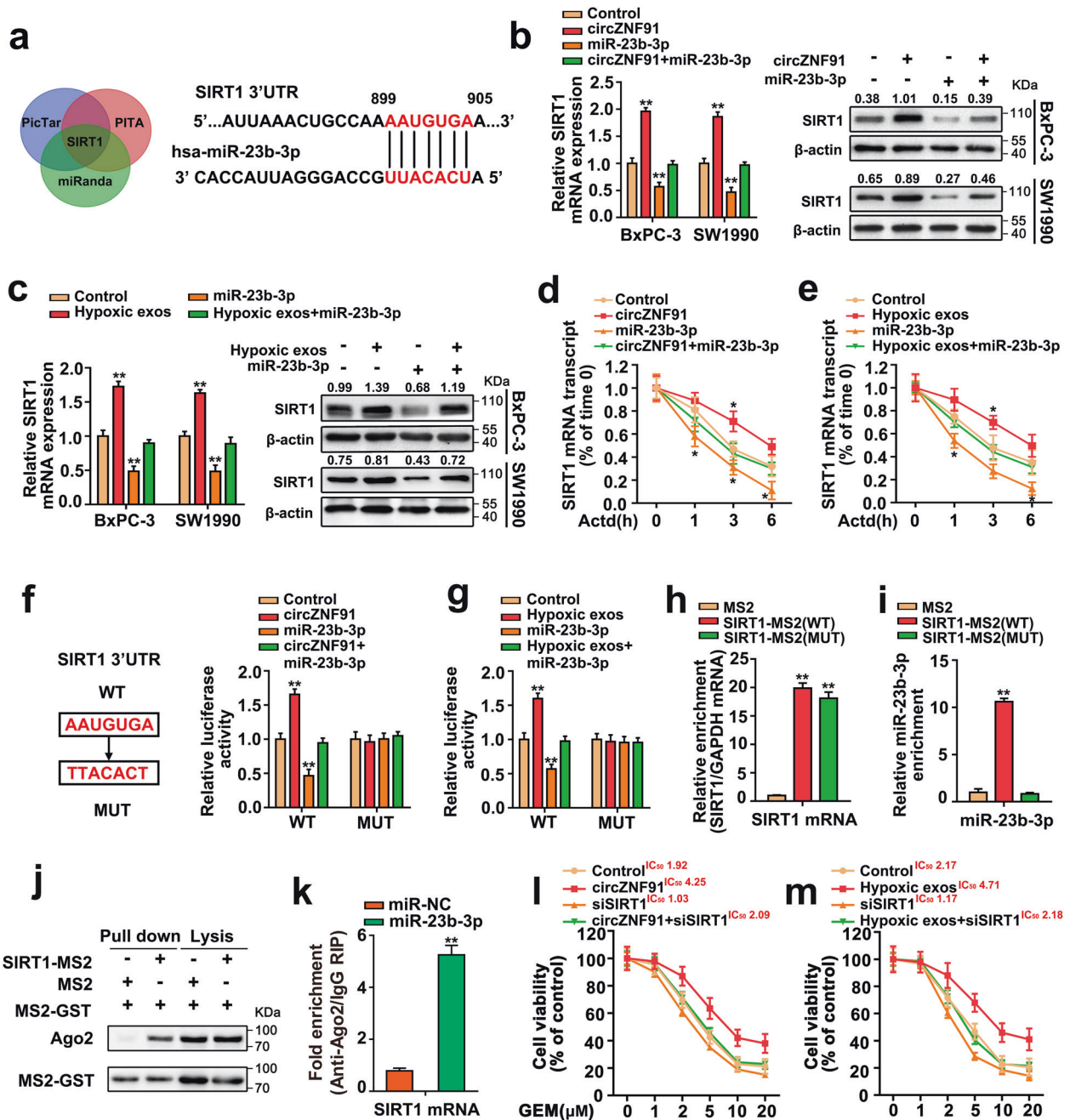


Fig. 3 CircZNF91 upregulates SIRT1 expression via competitively binding to miR-23b-3p. **a** (Left) Venn diagram presents SIRT1 as a predicted target of miR-23b-3p by PicTar, PITA, and miRanda. (Right) Sequence alignment predicted miR-23b-3p binding sites within the 3'UTR of SIRT1 mRNA. **b, c** RT-qPCR and western blot analysis of SIRT1 expression in circZNF91 overexpression (**b**) or hypoxic exosomes pre-incubated (**c**) BxPC-3/SW1990 cells with co-transfection of miR-23b-3p. **d, e** RT-qPCR assay of SIRT1 mRNA at indicated time point in circZNF91 overexpression (**d**) or hypoxic exosomes pre-incubated (**e**) BxPC-3/SW1990 cells with co-transfection of miR-23b-3p after treatment of ActD (1 μ g/mL). **f, g** (Left) The WT or MUT miR-23b-3p binding sites in 3'UTR of SIRT1 mRNA. (Right) Luciferase reporter assay in circZNF91 overexpression (**f**) or hypoxic exosomes pre-incubated (**g**) BxPC-3/SW1990 cells with co-transfection of miR-23b-3p after pre-transfection of WT or MUT plasmid. **h, i** RT-qPCR assay of SIRT1 mRNA (**h**) and miR-23b-3p (**i**) trapped by MS2 in BxPC-3 cells transfected with plasmid of MS2, SIRT1-MS2 (WT), or SIRT1-MS2 (MUT) for 48 h. **j** Western blot analysis of Ago2 protein in the MS2 trap assay. **k** RIP assay of SIRT1 transcripts enriched by Ago2 antibody in BxPC-3 cells transfected with miR-NC or miR-23b-3p mimic. **l, m** MTT assay detected the cell viability in circZNF91 overexpression (**l**) or hypoxic exosomes pre-incubated (**m**) BxPC-3 cells co-transfected with siSIRT1 followed by GEM treatment at indicated concentrations for 48 h. The value of IC₅₀ was shown as indicated. Results were shown as mean \pm SD of at least three independent experiments. * p < 0.05, ** p < 0.01.

the circZNF91/miR-23b-3p/SIRT1 pathway was involved in regulating HIF-1 α -associated glycolysis. Collectively, these data verified that HIF-1 α -promoted glycolysis was critically necessary for hypoxic exosomal circZNF91-transmitted GEM resistance in normoxic PC cells.

Exosomal circZNF91 is transcriptionally upregulated by HIF-1 α during hypoxic condition

Recent studies had shown that a subset of circRNAs were transcriptionally regulated by HIF-1 α during hypoxic condition [33]. Thereby, we presumed that the increased circZNF91 in hypoxic

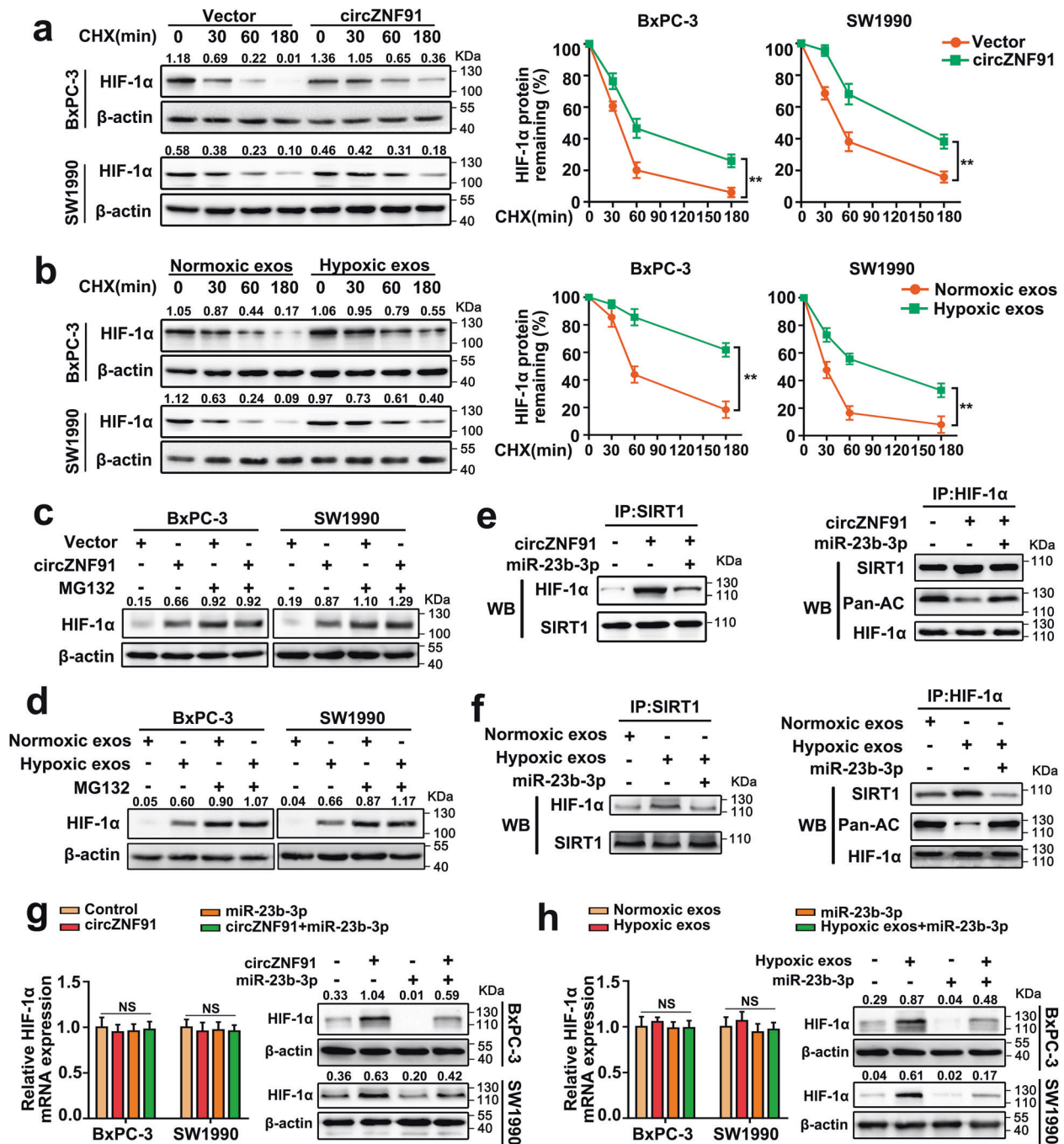


Fig. 4 Exosomal circZNF91 stabilizes HIF-1 α protein by SIRT1-dependent deacetylation. **a, b** After being cultured under hypoxia for 24 h, BxPC-3/SW1990 cells were transfected with plasmid of vector or circZNF91 or treated with normoxic exosomes or hypoxia exosomes for 48 h. We treated the transfected cells with cycloheximide (CHX, 50 μ g/mL) for periods of time as indicated. Then extracting the total proteins and analyzed the protein level of HIF-1 α by western blot. **c, d** Western blot assay analyzed the protein level of HIF-1 α in BxPC-3/SW1990 cells transfected with plasmid of vector or circZNF91 or treated with normoxic exosomes or hypoxia exosomes for 48 h with or without the absence of MG132 (20 μ M) for 3 h. **e, f** HIF-1 α , SIRT1, and Pan-AC protein level in circZNF91 overexpression (**e**) or hypoxia exosomes pre-incubated (**f**) BxPC-3 cells with co-transfection of miR-23b-3p mimic were analyzed in the cell lysates following anti-SIRT1 and anti-HIF-1 α immunoprecipitation. **g** RT-qPCR and western blot analysis of HIF-1 α mRNA and protein level in PC cells co-transfected with plasmid of circZNF91, miR-23b-3p mimic, or correlated control. **h** RT-qPCR and western blot analysis of HIF-1 α mRNA and protein level in PC cells pre-treated with normoxic or hypoxia exosomes, which followed by co-transfection with miR-23b-3p mimic or control. Results were shown as mean \pm SD of at least three independent experiments. ** p < 0.01.

exosomes might be attributed to HIF-1 α -regulated transcription. First, both the cellular and exosomal circZNF91 levels were obviously increased in PC cells during hypoxia in a time-dependent manner (Fig. 6a, b). Meanwhile, DNA sequence analysis indicated two potential hypoxia responsive elements (HREs) in promoter area of

ZNF91, the host gene of circZNF91. Moreover, the ChIP assay verified that only the region at -643 to -639 bp upstream of circZNF91 transcription start sites could bind to HIF-1 α , which could be enhanced during hypoxia (Fig. 6c). ChIP assay also revealed that the binding between RNA polymerase II and HRE of circZNF91 promoter

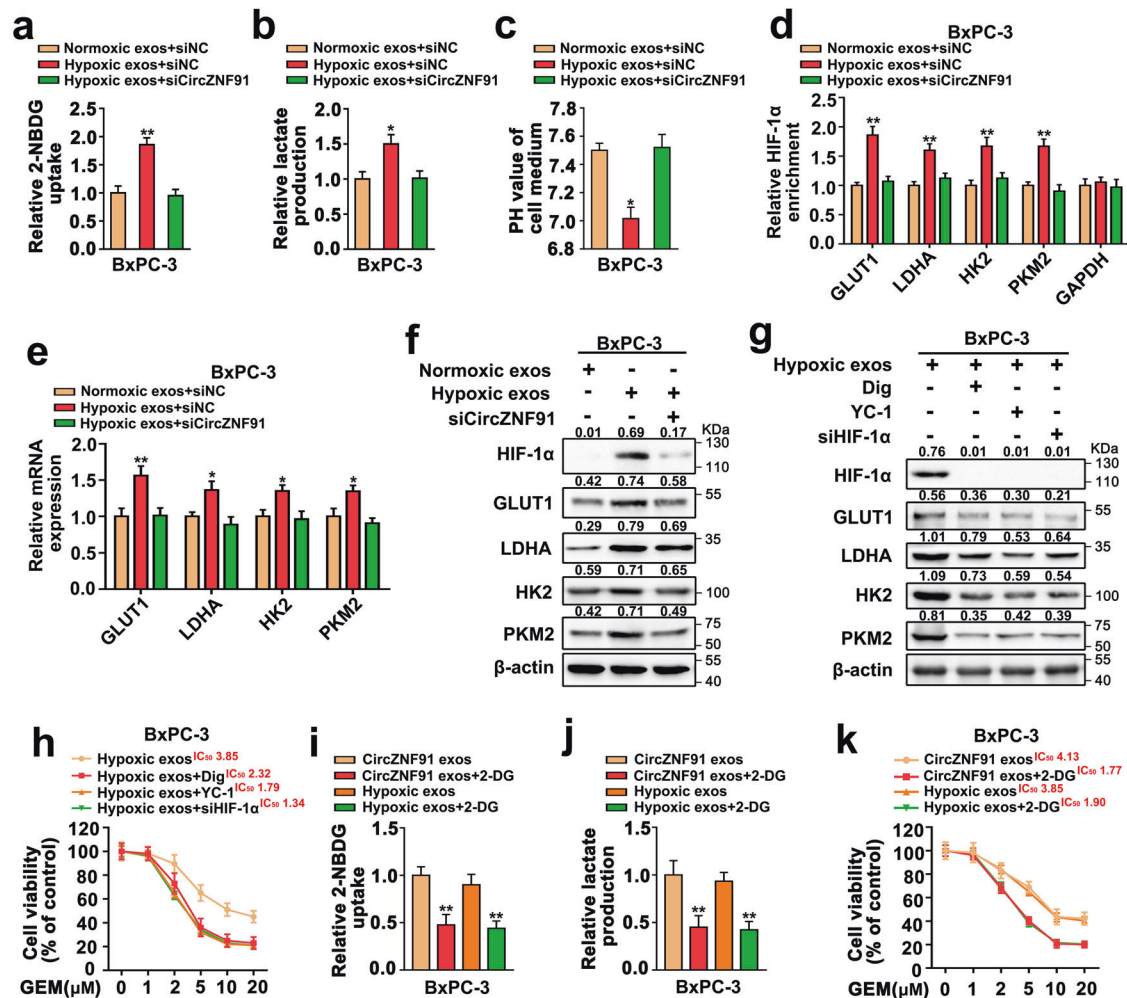


Fig. 5 Hypoxic exosomal circZNF91 promotes GEM resistance of normoxic PC cells by enhancing HIF-1 α -regulated glycolysis. **a–c** Glucose consumption, lactate production, and extracellular pH value of normoxic exosomes or hypoxic exosomes pre-incubated BxPC-3 cells that were transfected with siNC or siCircZNF91. **d** ChIP assay with anti-HIF-1 α antibody or IgG was conducted to explore the binding between HIF-1 α protein and the promoter of glycolytic enzymes (GLUT1, LDHA, HK2, and PKM2) in normoxic exosomes or hypoxic exosomes pre-incubated BxPC-3 cells transfected with siNC or siCircZNF91. **e** RT-qPCR analysis of GLUT1, LDHA, HK2, and PKM2 mRNA level in normoxic exosomes or hypoxic exosomes pre-incubated BxPC-3 cells transfected with siNC or siCircZNF91. **f** Western blot analysis of HIF-1 α , GLUT1, LDHA, HK2, and PKM2 protein level in normoxic exosomes or hypoxic exosomes pre-incubated BxPC-3 cells transfected with siNC or siCircZNF91. **g** Western blot analysis of HIF-1 α , GLUT1, LDHA, HK2, and PKM2 protein level in hypoxic exosomes pre-incubated BxPC-3 cells treated with Dig (100 nM)/YC-1 (100 μ M) or co-transfection of siNC or siHIF-1 α . **h** MTT assay detected the cell viability of hypoxic exosomes pre-incubated BxPC-3 cells treated with Dig (100 nM)/YC-1 (100 μ M) or co-transfected with siNC or siHIF-1 α followed by GEM treatment at indicated concentrations for 48 h. **i, j** Glucose consumption and lactate production of circZNF91 exosomes or hypoxic exosomes pre-incubated BxPC-3 cells treated with 2-DG (10 mM). **k** MTT assay detected the cell viability of circZNF91 exosomes or hypoxic exosomes pre-incubated BxPC-3 cells treated with 2-DG (10 mM) for 48 h followed by GEM treatment at indicated concentrations for 48 h. The value of IC₅₀ was shown as indicated. Results were shown as mean \pm SD of at least three independent experiments. * p < 0.05, ** p < 0.01.

was increased under hypoxia, which further confirmed that hypoxia activated transcription of circZNF91 (Fig. 6d). To validate the activation of HIF-1 α on circZNF91 promoter, circZNF91 promoter sequences containing HRE sequence (WT) or mutant HRE sequence (MUT) were inserted into a luciferase reporter vector and transfected into PC cells. Results of luciferase reporter assay demonstrated that the promoter activity of circZNF91 was significantly enhanced in WT but not MUT-transfected PC cells during hypoxia, while decreased after depletion of HIF-1 α (Fig. 6e). The results further verified that the hypoxia-induced increase of intracellular circZNF91 was obviously inhibited by depletion of HIF-1 α (Fig. 6f, g). Meanwhile, ActD, RNA polymerase II inhibitor, could partially reduce circZNF91 expression in PC cells treated with hypoxic exosomes (Fig. 6h), indicating that the increase of circZNF91 in recipient cells is not only derived from the transmission of hypoxic exosomes, but also induced by endogenous transcription. Besides, expressions of circZNF91 and glycolytic genes

were remarkably increased in recipient PC cells treated with hypoxic exosomes, but obviously inhibited by knockdown HIF-1 α (Fig. 6i, j). Therefore, these results further supported that circZNF91 transmitted into recipient PC cells further enhanced stabilization of HIF-1 α by depriving the inhibition of miR-23b-3p on SIRT1, which indirectly promoted endogenous transcription of circZNF91 and formed a positive feedback.

Targeting circZNF91/miR-23b-3p impedes the hypoxic exosome-promoted chemoresistance of PC in vivo

To further demonstrate the function of exosomal circZNF91 in transforming GEM resistance in vivo, we used BxPC-3 cells to construct xenograft nude mice models. The cells were subcutaneously injected into the right hip of nude mice. Then mixed liquor of purified exosomes and siCircZNF91/miR-23b-3p mimic was injected intratumorally every 3 days. And the mice were

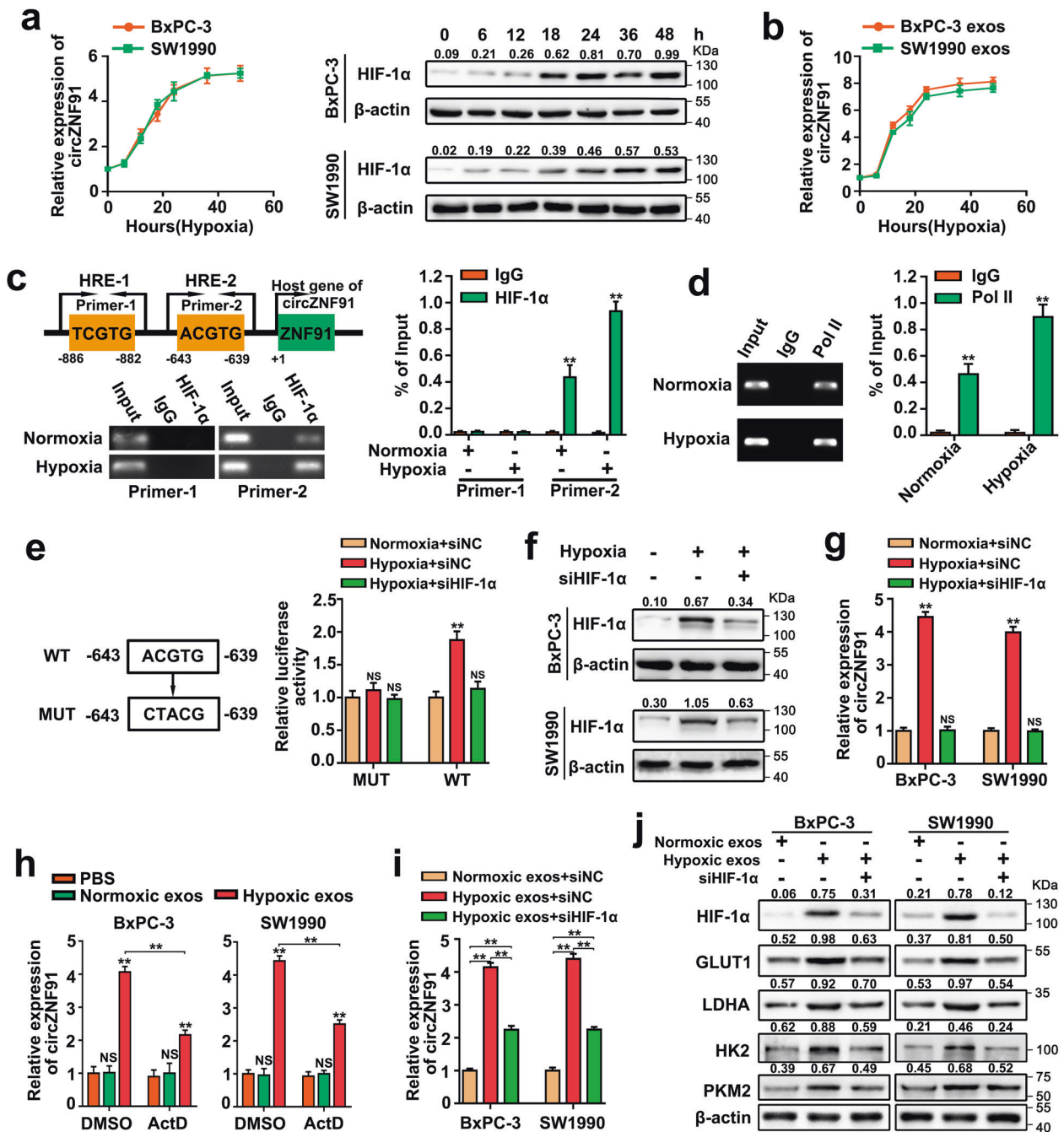


Fig. 6 Exosomal circZNF91 is transcriptionally upregulated by HIF-1 α during hypoxic condition. **a** (Left) RT-qPCR assay detected the level of circZNF91 in BxPC-3/SW1990 cells cultured under hypoxia for different time points. (Right) Western blot analysis of HIF-1 α protein level in BxPC-3/SW1990 cells exposed to different time of hypoxia. **b** RT-qPCR assay to detect exosomal circZNF91 expression in exosomes derived from BxPC-3/SW1990 cells exposed to different time of hypoxia. **c** Schematic illustration of circZNF91 promoter region and two HREs of potential HIF-1 α binding sites were shown. CHIP assay with anti-HIF-1 α antibody or IgG was conducted to explore the binding between HIF-1 α protein and HRE of circZNF91 promoter in BxPC-3 cells under normoxia and hypoxia. **d** CHIP assay with anti-Pol II antibody or IgG was conducted to test the binding between Pol II and circZNF91 promoter in BxPC-3 cells under normoxia and hypoxia. **e** (Left) The HRE-2 sequences were mutated as indicated. WT means "wild type" and MUT means "mutant type." (Right) CircZNF91 promoter activity was measured simultaneously in BxPC-3 cells cultured under normoxia or hypoxia and co-transfected with siNC or siHIF-1 α . **f** Western blot analysis of HIF-1 α protein level in BxPC-3/SW1990 cells cultured under normoxia or hypoxia and co-transfected with siNC or siHIF-1 α . **g** RT-qPCR assay to assess the level of circZNF91 in BxPC-3/SW1990 cells cultured under normoxia or hypoxia and co-transfected with siNC or siHIF-1 α . **h** RT-qPCR analysis of circZNF91 in BxPC-3 cells treated with ActD (1 μ g/ml) followed by treatment of PBS, normoxic exosomes, or hypoxic exosomes for 24 h. **i** RT-qPCR assay to assess the level of circZNF91 in BxPC-3/SW1990 cells incubated with exosomes, derived from BxPC-3/SW1990 cells cultured under normoxia or hypoxia, and co-transfected with siNC or siHIF-1 α . **j** Western blot analysis of HIF-1 α , GLUT1, LDHA, HK2, and PKM2 protein level in BxPC-3/SW1990 cells incubated with exosomes, derived from BxPC-3/SW1990 cells cultured under normoxia or hypoxia, and co-transfected with siNC or siHIF-1 α . Results were shown as mean \pm SD of at least three independent experiments. ** p < 0.01.

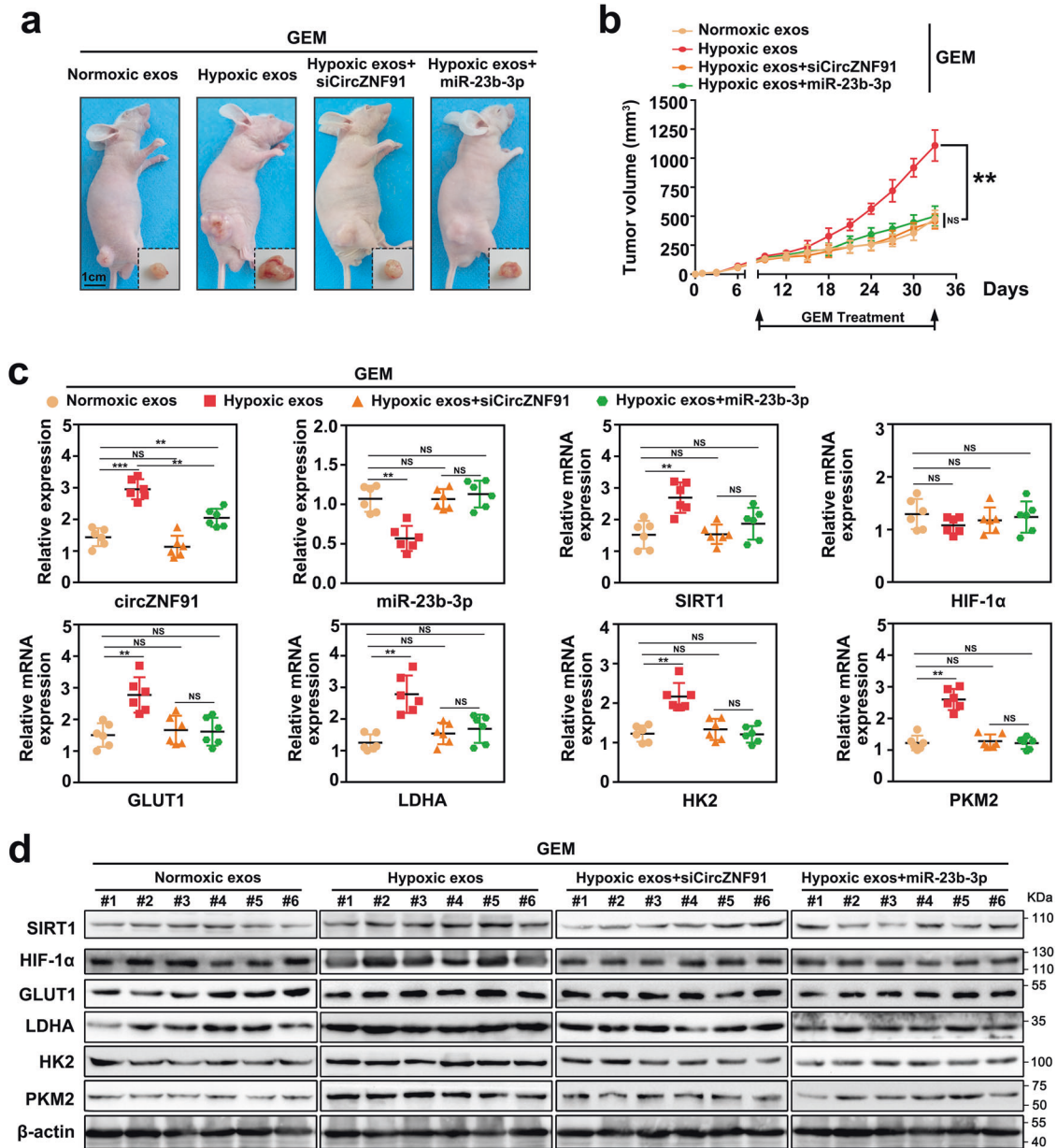


Fig. 7 Targeting circZNF91/miR-23b-3p impedes the hypoxic exosome-promoted chemoresistance of PC in vivo. **a** Xenograft tumor of nude mice injected with BxPC-3 cells for 1 week followed by injection of purified exosomes, mixed with siCircZNF91 or miR-23b-3p mimic every 3 days. And the mice were treated with GEM biweekly. $N = 6$. Scale bar: 1 cm. **b** The tumor volume of nude mice was measured using the formula $V = (W^2 \times L)/2$ for caliper measurements every 3 days. V is tumor volume, W is tumor width, L is tumor length. **c** RT-qPCR assay analyzed circZNF91, miR-23b-3p expression, and the mRNA level of SIRT1, HIF-1 α , GLUT1, LDHA, HK2, and PKM2 in xenograft tumors. **d** Western blot assays showed the SIRT1, HIF-1 α , GLUT1, LDHA, HK2, and PKM2 protein level in the subcutaneous tumors. Results were shown as mean \pm SD. ** $p < 0.01$, *** $p < 0.001$.

treated with GEM simultaneously. Result showed that mice injected with hypoxic exosomes exhibited a poorer GEM response than those injected with normoxic exosomes. Importantly, intratumor injection of hypoxic exosomes with siCircZNF91 or miR-23b-3p mimic restored the sensitivity of xenografts to GEM (Fig. 7a, b). The RT-qPCR analysis displayed an increased expression of circZNF91 in tumors injected with hypoxic exosomes with or without miR-23b-3p (Fig. 7c). It was also observed that miR-23b-3p expression was significantly decreased in tumors injected with hypoxic exosomes, which was rescued by circZNF91 knockdown and miR-23b-3p upregulation. Meanwhile, mRNA level of SIRT1 and glycolytic genes were increased in tumors injected with hypoxic exosomes, which was reversed by circZNF91 knockdown

and miR-23b-3p upregulation, and the mRNA level of HIF-1 α had no change. In addition, both western blot and immunohistochemistry (IHC) assays displayed that expressions of SIRT1, HIF-1 α , and glycolytic genes were upregulated in tumors treated with hypoxic exosomes, which was restored by circZNF91 knockdown and miR-23b-3p upregulation (Fig. 7d and Supplementary Fig. S9a, b). Meanwhile, the results showed that the proliferation of cells was slightly enhanced by hypoxic exosome and circZNF91 overexpression, and reversed by siCircZNF91 and miR-23b-3p overexpression, respectively (Supplementary Fig. S9c, d). Thus, the results above elucidated that circZNF91/miR-23b-3p was a potential target for treatment of GEM resistance and proliferation.

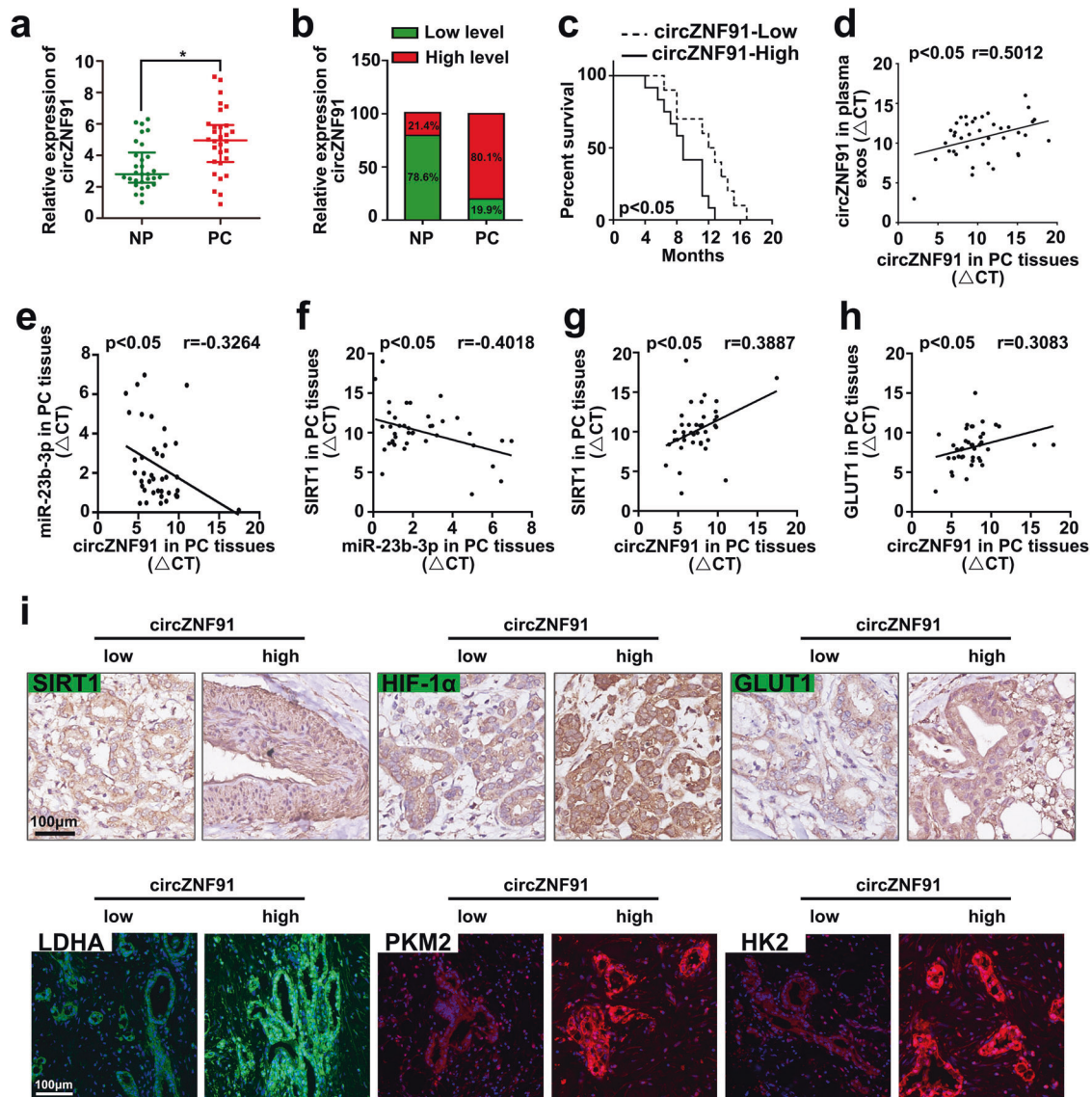


Fig. 8 CircZNF91 is overexpressed in PC tissues and associated with poor prognosis. **a, b** RT-qPCR analysis of circZNF91 in tissues of NP patients and PC patients ($n = 40$). PC patients whose circZNF91 expression level was lower or higher than the median value were classified into low or high level of circZNF91 groups. **c** Kaplan–Meier curves analysis of percentage survival of 40 patients in the high and low circZNF91 groups. CircZNF91 expression was categorized into “high” and “low” using the median value as the cutoff point. **d** Pearson correlation analysis between circZNF91 levels in plasma exosomes and PC tissues determined by RT-qPCR. **e–h** Pearson correlation analysis between circZNF91 and miR-23b-3p (**e**), SIRT1 and miR-23b-3p (**f**), SIRT1 and circZNF91 (**g**), GLUT1 and circZNF91 (**h**) in PC tissues determined by RT-qPCR. **i** Representative images of IHC and IF assays showed the SIRT1, HIF-1 α , GLUT1, LDHA, HK2, and PKM2 protein level in high and low circZNF91 level PC tissues. Scale bar: 100 μ m. * $p < 0.05$.

CircZNF91 is overexpressed in PC tissues and associated with poor prognosis

To demonstrate clinical relevance of circZNF91, we detected circZNF91 expression in the paired non-tumor peritumoral (NP) tissues, PC tissues, and plasma of PC patients. Expression of circZNF91 was evidently increased in PC tissues (Fig. 8a, b). PC patients with increased expression of circZNF91 presented shorter overall survival compared with those with less expression of circZNF91 (Fig. 8c). In addition, circZNF91 expression in PC tumors was correlated with those in plasma exosomes of PC patients (Fig. 8d). Results further showed that circZNF91 and miR-23b-3p had a negative correlation in our PC tissues (Fig. 8e). We also found that mRNA level of SIRT1 was positively correlated with circZNF91, but negatively correlated with miR-23b-3p in PC tissues (Fig. 8f, g). Meanwhile, it was observed that the mRNA level of GLUT1 was positively correlated with

circZNF91 (Fig. 8h). IHC/immunofluorescence (IF) analysis showed that SIRT1, HIF-1 α , and glycolytic enzymes were highly expressed in PC tissues with high expression of circZNF91 (Fig. 8i). Therefore, these data indicated that HIF-1 α /circZNF91/miR-23b-3p pathway was involved in tumorigenesis of PC.

DISCUSSION

The expression of HIF-1 α increases under hypoxia, which is the adaptive response of tumor cells to hypoxia. Studies have shown that overexpression of HIF-1 α in human solid tumors is closely correlated with the tumor’s chemotherapy resistance [12], of which the mechanism is mostly focused on changes in intracellular signaling pathways [34]. However, the crosstalk between hypoxic and normoxic cancer cells is ambiguous. Here, we found that hypoxia might induce PC cells to release circZNF91-enriched

exosomes, which could distribute to normoxia and then facilitate the transition of normoxic PC cells to hypoxia phenotype with increasing glycolysis and chemotherapy resistance. Along with previous report, our study indicated a critical role of exosomes in the interaction between tumor cells locating in heterogeneous microenvironment, transmitting chemoresistance of hypoxic PC cells to normoxic PC cells.

Hypoxia-induced intracellular proteins and ncRNAs affect tumor microenvironment and chemoresistance of cancer cells through exosomal secretion. Research had elucidated that exosomes, derived from non-small-cell lung cancer cell cultured under hypoxia, contributed to cisplatin resistance of cancer cells cultured under normoxia via transmitting miR-21 [35]. In addition, Patel et al. discovered that exosomes secreted by hypoxic cancer cells enhanced chemoresistance of hepatocellular carcinoma cells to sorafenib, and doxorubicin through delivering linc-RoR [36]. However, the role of circRNAs in transmission of drug resistance through exosomes between hypoxic and normoxic cells is rarely studied. CircRNA microarray was performed to validate circRNA abnormally expressed in hypoxic exosomes. Among those upregulated circRNAs, only circZNF91 had been identified as a functional circRNA, containing 24 target sites for miR-23b-3p and playing important roles in keratinocyte differentiation [23]. Meanwhile, miR-23b-3p had been reported to play important roles in numerous carcinomas including PC [37], gastric cancer [38], and lung cancer [39]. Thereby, we presumed that exosomal circZNF91 might contribute to chemoresistance transition between hypoxic PC cells and normoxic PC cells. Meanwhile, through *in vitro* and *in vivo* experiments, we found that hypoxia-induced exosomal circZNF91 had a critical role in regulating chemoresistance of normoxic PC cells to GEM. Certainly, hypoxic exosomes must also contain other circRNAs with the same biological effects, which will be discovered and verified in future studies.

We further revealed the potential mechanism of exosomal circZNF91 promoting chemoresistance of normoxic cells. According to the reported sequencing data, we found that circZNF91 has multiple miRNA binding sites. Through molecular biology experiments, we selected miR-23b-3p as target of circZNF91. It has been reported that circZNF91 played an important role in keratinocyte differentiation through targeting miR-23b-3p [23]. In our studies, we found that circZNF91 sponged miR-23b-3p to elevate SIRT1 expression, which mediate HIF-1 α stabilization via deacetylation [29]. Under hypoxia, tumor cells overexpress HIF-1 α to promote transcription of downstream target genes to adapt to changes in tumor microenvironment and improve the tolerance of tumor cells to chemotherapy. Glycolysis in tumors could be driven by HIF-1 α stabilization, independently of hypoxic environment [40]. HIF-1 α activates a number of glycolytic protein isoforms and upregulates gene coding for glucose transporter such as Glut-1 and enzymes of glycolytic pathway [41]. Studies have reported that inhibiting glycolysis can more effectively kill tumor cells that are resistant to chemotherapeutics under hypoxia [42]. Therefore, we suspect that circZNF91 promotes drug resistance via promoting HIF-1 α -driven glycolysis. The results showed that inhibiting HIF-1 α or glycolysis could reverse the chemoresistance mediated by hypoxic exosomal circZNF91. Furthermore, the results *in vivo* indicated that targeting circZNF91 could enhance chemosensitivity of PC. Thereafter, our study revealed that circZNF91 was involved in the hypoxic exosome-promoted glycolysis and chemoresistance of normoxic PC cells to GEM.

Recent studies have revealed that non-coding RNAs were induced during hypoxia [43]. HREs contained in promoter regions of hypoxia responsive genes can be bound to HIF-1 α , and hypoxia can improve the affinity of such a complex thereby promoting the transcription of hypoxia responsive genes. There are two putative HREs in promoter area of circZNF91. The ChIP and luciferase reporter assay validated the binding between HIF-1 α and HRE of circZNF91 promoter, which was promoted during hypoxic

condition. After knockdown HIF-1 α in hypoxic PC cells, the increased expression of intracellular circZNF91, induced by hypoxia, was obviously reversed. In addition, inhibition of RNA transcription could partially reduce the increased circZNF91 expression induced by hypoxic exosomes, suggesting that hypoxic exosomes may further induce the endogenous circZNF91 expression in recipient PC cells to augment the effect. Moreover, expressions of circZNF91 and glycolytic genes were remarkably increased in recipient PC cells treated with hypoxic exosomes, which could be obviously inhibited by HIF-1 α knockdown. In summary, our results indicate that circZNF91 is regulated by HIF-1 α at transcription level, forming a reciprocal feedback.

Our research implicated that hypoxic PC cells could activate hypoxic signals of distant cancer cells in normoxia. CircZNF91 was enriched in exosomes derived from hypoxic PC cells, which was essential for the promoted glycolysis and chemoresistance of normoxic PC cells. We further revealed that hypoxia-induced circZNF91 in exosomes was transcriptionally regulated by HIF-1 α . Nevertheless, hypoxic exosome-derived circZNF91 sponged miR-23b-3p to elevate SIRT1 expression, which contributed to deacetylation-dependent stabilization of HIF-1 α protein of normoxic PC cells.

MATERIALS AND METHODS

Patient samples

Forty pairs of PC tissues, matched paracancerous tissues, and blood samples were obtained from Pancreatic Disease Institute of Union Hospital (Wuhan, China) between May 2015 and May 2016 from patients undergoing surgical treatment. Tissues were either formalin fixed and paraffin embedded or snap frozen. Ethics Committee of Academic Medical Center of Huazhong University of Science and Technology approved this study (Permission No: 2013, S199). The informed consent was obtained from all PC patients.

Microarray

This method was the similar as in our previous article [44]. First, we cultured cells under hypoxia and normoxia for 48 h with exosome-free FBS medium and extracted exosomes in the culture medium. Then the extracted exosomes were taken for Microarray (KangChen Bio-tech, Shanghai, China). Total RNA of exosomes was extracted. Nanodrop was applied to measure total RNA concentration and evaluate RNA purity. Process the RNA with RNase R to remove linear RNA and enrich circRNAs after quality inspection. The circRNAs were then specifically and efficiently labeled using a random primer labeling method (Arraystar Super RNA Labeling Kit, Arraystar Inc). Hybridize the labeled circRNAs with Arraystar Human circRNA Microarray Version 2.0 (8 \times 15 K, Arraystar Inc). The array was scanned with Agilent scanner G2505C after washing the slides. Analyze the acquired array image using Agilent feature extraction software (version 11.0.1.1). Use R software package (R version 3.1.2) to perform quantile normalization and subsequent data processing.

Supplementary methods

The methods of cell culture, exosome isolation and treatment, cell viability, MS2-GST pulldown, plasmids and siRNA transfection, RT-qPCR, western blot, IHC/IF, Luciferase reporter assay, ChIP, RIP, Co-IP, biotin-based pulldown, RNA-FISH, detection of glucose uptake, lactate and PH value of cell medium, xenograft assay, and statistical analysis are available in Supplementary materials. The sequence of CircZNF91 (Supplementary Table S1), sequence of mutant circZNF91 (Supplementary Table S2), sequence of siRNA, mimic, and inhibitor (Supplementary Table S3), vector structure of overexpression plasmid (Supplementary Table S4), sequence of PCR primers (Supplementary Table S5), and sequence of probes (Supplementary Table S6) are also available in Supplementary materials.

REFERENCES

1. Siegel RL, Miller KD, Jemal A. Cancer statistics, 2020. *CA Cancer J Clin.* 2020;70:7–30.
2. Christenson ES, Jaffee E, Azad NS. Current and emerging therapies for patients with advanced pancreatic ductal adenocarcinoma: a bright future. *Lancet Oncol.* 2020;21:e135–45.

3. Klotz R, Doerr-Harim C, Ahmed A, Tjaden C, Tarpey M, Diener MK, et al. Top ten research priorities for pancreatic cancer therapy. *Lancet Oncol.* 2020;21:e295–6.
4. Hosein AN, Brekken RA, Maitra A. Pancreatic cancer stroma: an update on therapeutic targeting strategies. *Nat Rev Gastroenterol Hepatol.* 2020;17:487–505.
5. Paulson AS, Tran CH, Tempero MA, Lowy AM. Therapeutic advances in pancreatic cancer. *Gastroenterology.* 2013;144:1316–26.
6. Da CWJ, Tran CH, Massarweh NN. Neoadjuvant treatment for patients with localized pancreatic adenocarcinoma: are we there yet? *Jama Oncol.* 2020;6:1163–4.
7. Bednar F, Pasca DMM. Chemotherapy and tumor evolution shape pancreatic cancer recurrence after resection. *Cancer Disco.* 2020;10:762–4.
8. Halbrook CJ, Pontious C, Kovalenko I, Lapienyte L, Dreyer S, Lee HJ, et al. Macrophage-released pyrimidines inhibit gemcitabine therapy in pancreatic cancer. *Cell Metab.* 2019;29:1390–9.
9. Karasic TB, O'Hara MH, Loaiza-Bonilla A, Reiss KA, Teitelbaum UR, Borazanci E, et al. Effect of gemcitabine and nab-paclitaxel with or without hydroxychloroquine on patients with advanced pancreatic cancer: a phase 2 randomized clinical trial. *Jama Oncol.* 2019;5:993–8.
10. Yokoi K, Fidler IJ. Hypoxia increases resistance of human pancreatic cancer cells to apoptosis induced by gemcitabine. *Clin Cancer Res.* 2004;10:2299–306.
11. Doktorova H, Hrabeta J, Khalil MA, Eckschlagler T. Hypoxia-induced chemoresistance in cancer cells: the role of not only HIF-1. *Biomed Pap.* 2015;159:166–77.
12. Warfel NA, El-Deiry WS. HIF-1 signaling in drug resistance to chemotherapy. *Curr Med Chem.* 2014;21:3021.
13. Rohwer N, Cramer T. Hypoxia-mediated drug resistance: novel insights on the functional interaction of HIFs and cell death pathways. *Drug Resist Updat.* 2011;14:191–201.
14. Jing X, Yang F, Shao C, Wei K, Xie M, Shen H, et al. Role of hypoxia in cancer therapy by regulating the tumor microenvironment. *Mol Cancer.* 2019;18:157.
15. Shukla SK, Purohit V, Mehla K, Gunda V, Chaika NV, Vernucci E, et al. MUC1 and HIF-1 α signaling crosstalk induces anabolic glucose metabolism to impart gemcitabine resistance to pancreatic cancer. *Cancer Cell.* 2017;32:71–87.
16. Lane JS, Hoff DV, Cridebring D, Goel A. Extracellular vesicles in diagnosis and treatment of pancreatic cancer: current state and future perspectives. *Cancers (Basel).* 2020;12:1530.
17. Ding C, Yi X, Wu X, Bu X, Wang D, Wu Z, et al. Exosome-mediated transfer of circRNA CircNFIX enhances temozolomide resistance in glioma. *Cancer Lett.* 2020;479:1–12.
18. Wang X, Zhang H, Yang H, Bai M, Ning T, Deng T, et al. Exosome-delivered circRNA promotes glycolysis to induce chemoresistance through the miR-122-PKM2 axis in colorectal cancer. *Mol Oncol.* 2020;14:539–55.
19. Icard P, Shulman S, Farhat D, Steyaert JM, Alifano M, Lincet H. How the Warburg effect supports aggressiveness and drug resistance of cancer cells? *Drug Resist Updat.* 2018;38:1–11.
20. Lin SC, Chien CW, Lee JC, Yeh YC, Hsu KF, Lai YY, et al. Suppression of dual-specificity phosphatase-2 by hypoxia increases chemoresistance and malignancy in human cancer cells. *J Clin Invest.* 2011;121:1905–16.
21. Ostrowski M, Carmo NB, Krumeich S, Fangeit I, Raposo G, Savina A, et al. Rab27a and Rab27b control different steps of the exosome secretion pathway. *Nat Cell Biol.* 2010;12:19–30. 1–13
22. Trajkovic K, Hsu C, Chiantia S, Rajendran L, Wenzel D, Wieland F, et al. Ceramide triggers budding of exosome vesicles into multivesicular endosomes. *Science.* 2008;319:1244–7.
23. Kristensen LS, Okholm T, Venø MT, Kjems J. Circular RNAs are abundantly expressed and upregulated during human epidermal stem cell differentiation. *RNA Biol.* 2018;15:280–91.
24. Yoon JH, Srikantan S, Gorospe M. MS2-TRAP (MS2-tagged RNA affinity purification): tagging RNA to identify associated miRNAs. *Methods.* 2012;58:81–7.
25. Oon CE, Strell C, Yeong KY, Ostman A, Prakash J. SIRT1 inhibition in pancreatic cancer models: contrasting effects in vitro and in vivo. *Eur J Pharm.* 2015;757:59–67.
26. Zhang JG, Hong DF, Zhang CW, Sun XD, Wang ZF, Shi Y, et al. Sirtuin 1 facilitates chemoresistance of pancreatic cancer cells by regulating adaptive response to chemotherapy-induced stress. *Cancer Sci.* 2014;105:445–54.
27. Zhou W, Xu J, Wang C, Shi D, Yan Q. miR-23b-3p regulates apoptosis and autophagy via suppressing SIRT1 in lens epithelial cells. *J Cell Biochem.* 2019;120:19635–46.
28. Borji M, Nourbakhsh M, Shafiee SM, Owji AA, Abdolvahabi Z, Hesari Z, et al. Down-regulation of SIRT1 expression by miR-23b contributes to lipid accumulation in HepG2 cells. *Biochem Genet.* 2019;57:507–21.
29. Joo HY, Yun M, Jeong J, Park ER, Shin HJ, Woo SR, et al. SIRT1 deacetylates and stabilizes hypoxia-inducible factor-1 α (HIF-1 α) via direct interactions during hypoxia. *Biochem Biophys Res Commun.* 2015;462:294–300.
30. Harris AL. Hypoxia—a key regulatory factor in tumour growth. *Nat Rev Cancer.* 2002;2:38–47.
31. Zhang H, Qian DZ, Tan YS, Lee K, Gao P, Ren YR, et al. Digoxin and other cardiac glycosides inhibit HIF-1 α synthesis and block tumor growth. *Proc Natl Acad Sci USA.* 2008;105:19579–86.
32. Yeo EJ, Chun YS, Cho YS, Kim J, Lee JC, Kim MS, et al. YC-1: a potential anticancer drug targeting hypoxia-inducible factor 1. *J Natl Cancer Inst.* 2003;95:516–25.
33. Boeckel JN, Jae N, Heumuller AW, Chen W, Boon RA, Stellos K, et al. Identification and characterization of hypoxia-regulated endothelial circular RNA. *Circ Res.* 2015;117:884–90.
34. Abraham J, Salama NN, Azab AK. The role of P-glycoprotein in drug resistance in multiple myeloma. *Leuk Lymphoma.* 2015;56:26–33.
35. Dong C, Liu X, Wang H, Li J, Dai L, Li J, et al. Hypoxic non-small-cell lung cancer cell-derived exosomal miR-21 promotes resistance of normoxic cell to cisplatin. *Oncotargets Ther.* 2019;12:1947–56.
36. Takahashi K, Yan IK, Kogure T, Haga H, Patel T. Extracellular vesicle-mediated transfer of long non-coding RNA ROR modulates chemosensitivity in human hepatocellular cancer. *Febs Open Bio.* 2014;4:458–67.
37. Wang P, Zhang J, Zhang L, Zhu Z, Fan J, Chen L, et al. MicroRNA 23b regulates autophagy associated with radioresistance of pancreatic cancer cells. *Gastroenterology.* 2013;145:1133–43. e1112
38. An Y, Zhang Z, Shang Y, Jiang X, Dong J, Yu P, et al. miR-23b-3p regulates the chemoresistance of gastric cancer cells by targeting ATG12 and HMGB2. *Cell Death Dis.* 2015;6:e1766.
39. Wang J, Xue H, Zhu Z, Gao J, Zhao M, Ma Z. Expression of serum exosomal miR-23b-3p in non-small cell lung cancer and its diagnostic efficacy. *Oncol Lett.* 2020;20:30.
40. Robey IF, Lien AD, Welsh SJ, Baggett BK, Gillies RJ. Hypoxia-inducible factor-1 α and the glycolytic phenotype in tumors. *Neoplasia.* 2005;7:324–30.
41. Semenza GL. HIF-1: upstream and downstream of cancer metabolism. *Curr Opin Genet Dev.* 2010;20:51–6.
42. Xu RH, Pelicano H, Zhou Y, Carew JS, Feng L, Ballala KN, et al. Inhibition of glycolysis in cancer cells: a novel strategy to overcome drug resistance associated with mitochondrial respiratory defect and hypoxia. *Cancer Res.* 2005;65:613–21.
43. Cho HS, Han TS, Hur K, Ban HS. The roles of hypoxia-inducible factors and non-coding RNAs in gastrointestinal cancer. *Genes (Basel).* 2019;10:1008.
44. Zeng Z, Xu F, Zheng H, Cheng P, Chen Q, Ye Z, et al. LncRNA-MTA2TR functions as a promoter in pancreatic cancer via driving deacetylation-dependent accumulation of HIF-1 α . *Theranostics.* 2019;9:5298–314.

ACKNOWLEDGEMENTS

The National Science Foundation Committee of China (Grant Number: 81372666, 81672406 to GZ; 81802450 to SZ; 81802377 to YN); and Clinical Research Physician Program of Tongji Medical College, Huazhong University of Science and Technology to GZ supported this study.

AUTHOR CONTRIBUTIONS

Designed and supervised the research: GZ. Performed cellular experiments: ZZ, YZ, SZ, ZY, YH, FX, JT, FW,SH and MH. Conducted animal experiments: ZZ, YZ, SZ. Provided the clinical data: QYC, YN, PH, DC, PX, JC, CH and CYW. Analyzed the data: GZ and ZZ. Wrote the manuscript: GZ and ZZ.

COMPETING INTERESTS

The authors declare no competing interests.

ADDITIONAL INFORMATION

Supplementary information The online version contains supplementary material available at <https://doi.org/10.1038/s41388-021-01960-w>.

Correspondence and requests for materials should be addressed to G.Z.

Reprints and permission information is available at <http://www.nature.com/reprints>

Publisher's note Springer Nature remains neutral with regard to jurisdictional claims in published maps and institutional affiliations.